Arnal Pastor, MP.; Perez Garnes, M.; Monleón Pradas, M.; Vallés Lluch, A. (2016). Topologically controlled hyaluronan-based gel coatings of hydrophobic grid-like scaffolds to modulate drug delivery. Colloids and Surfaces B Biointerfaces. 140:412-420. https://doi.org/10.1016/j.colsurfb.2016.01.004

TOPOLOGICALLY CONTROLLED HYALURONAN-BASED GEL COATINGS OF HYDROPHOBIC GRID-LIKE SCAFFOLDS TO MODULATE DRUG DELIVERY

M. Arnal-Pastor[1, #], M. Pérez-Garnes[1,#], M. Monleón Pradas[1,2], A. Vallés Lluch[1,*]

[1]*Center for Biomaterials and Tissue Engineering, Universitat Politècnica de València, C. de Vera s/n, 46022, Valencia, Spain*

[2]*Networking Research Center on Bioengineering, Biomaterials and Nanomedicine, Valencia, Spain*

 # Equal contribution

**Corresponding author. Tel.: +3496387000; fax: +34963877276. E-mail: avalles@ter.upv.es*

Statistical summary

6000 words

7 figures

0 tables

Abstract

Scaffolds based on poly(ethyl acrylate) having interwoven channels were coated with a hyaluronan (HA) hydrogel to be used in tissue engineering applications. Controlled typologies of coatings evolving from isolated aggregates to continuous layers, which eventually clog the channels, were obtained by using hyaluronan solutions of different concentrations. The efficiency of the HA loading was determined using gravimetric and thermogravimetric methods, and the hydrogel loss during the subsequent crosslinking process was quantified, seeming to depend on the mass fraction of hyaluronan initially incorporated to the pores. The effect of the topologically different coatings on the scaffolds, in terms of mechanical properties and swelling at equilibrium under different conditions was evaluated and correlated with the hyaluronan mass fraction. The potential of these hydrogel coatings as vehicle for controlled drug release from the scaffolds was validated using a protein model.

Keywords: hyaluronan; poly(ethyl acrylate); scaffold; hydrogel coating; controlled release

1. Introduction

Polymer-based materials have been widely investigated for tissue engineering applications for their versatility in terms of chemical, physical and mechanical properties and ease of handling to obtain microporous structures. Among them, poly(ethyl acrylate) (PEA) is a biostable polymer with good biocompatibility with cells such as chondrocytes [1], osteoblasts [2], endothelial cells [3], keratinocytes [4], neural cells [5-8] or dental pulp stem cells [9], and has been proposed as a feeder-free platform for the maintenance and growth of embryonic stem cells [10]. Its scaffolds have been implanted in several tissues with regenerative purposes [5,11-13]. They can be manufactured in a variety of pore architectures including aligned [14] and interwoven [15] microchannels and interconnected microspheres [16] by using porogen leaching techniques. These scaffolds can be further combined with others of dissimilar nature: for example, in [15, 16] the authors combined them with a self-assembling peptide gel as filling in their pores. The inclusion of a hydrogel improves cell colonization and maintenance in the pores.

PEA undergoes its vitreous transition around -10ºC, so it shows a rubbery behavior at physiological temperatures [17], characterized by being softer and more elastic than other similar polymers. As grid-like scaffolds with pores diameter of 150 microns and porosity of 76.4 ± 6.1%, its Young's modulus decreases from 0.84±0.08 MPa for bulk PEA to 0.04±0.02 MPa [13]. It's density is 1.13 gcm^{-3} [18]. Additionally, PEA is a hydrophobic polymer and the amorphous networks thereof result in low water uptake (equilibrium water content in PBS of 1.14±0.16% [13]), thus maintaining their size and shape stable in aqueous environments. PEA has been shown to favor the adhesion of proteins such as fibronectin [2, 19] and to induce its spontaneous fibrillogenesis, due to the particular mobility and polarity of its side chain, together with its low wettability. These peculiarities encourage its use for soft tissue engineering purposes.

Hyaluronic acid, usually referred to as its sodium salt form, hyaluronan (HA), is a natural polymer of the glycosaminoglycans family that forms part of the extracellular matrix of several tissues. HA contains binding sites for extracellular, intracellular and transmembrane proteins, known as hyaladherins [20]. Additionally, HA molecules possess physical properties and regulate cell signaling pathways in a size-dependent manner [21]: high molecular weight HA at physiological conditions behaves as a viscoelastic material, increases hydration and displays anti-inflammatory properties, whereas low molecular weight HA up-regulates important cell functions implied in the regenerative process including proliferation, migration, angiogenesis and the immune response.

In spite of its biological interest and degradation by-products, HA has an important drawback: it shows a short residence time in physiological conditions (because of its high solubility) and a fast degradation rate, as well as an excessively low structural stability to be shaped as scaffold for cell support and ingrowth. For these reasons, HA is usually crosslinked [22,23] or modified [24]. Several HA-based hydrogels have indeed been proposed in the tissue engineering field and, in particular, HA crosslinked with divinyl sulfone (HA-DVS) constitutes one of the most studied, with clinical applications such as intra-cutaneous injections as dermal fillers [25] and intra-articular injections for osteoarthritis [26]. HA-based hydrogels give rise to stable and more easy handling structures with large hydration, exhibiting great diffusion of substances implied in cell survival. They have thus been used alone to develop scaffolds [27] and drug and cell carriers [28-31].

Herein, the HA-DVS crosslinking reaction was performed inside the interwoven channels of hydrophobic PEA scaffolds, resulting in a combined material of peculiar properties and potential applications: the hydrogel as coating provides an artificial and more cell-friendly nanoenvironment, and the good biocompatibility and better mechanical stability of PEA joins the biological benefits and high hydration rates of HA-DVS hydrogel. This work ensues from

a previous one [32], which addressed the problems faced to produce different HA coating typologies and to characterize their physical state in the scaffold-coating construct. Firstly, the efficiency of the coating procedure using solutions with different HA concentrations has been assessed, as well as the efficiency of the crosslinking reaction within the microchannels with DVS. Next, the morphology of the coating in the dry and swollen state, its water uptake under diverse conditions and its effect on the mechanical properties of the ensemble have been studied and correlated with the initial HA solution used to produce the coating. Finally, the ability of the HA-DVS hydrogels to absorb and release molecules from the micropores of the hydrophobic scaffolds has been followed with bovine serum protein (BSA) used as protein model.

2. Materials and methods

2.1. Scaffolds preparation

Scaffolds were prepared as described in [33]. Briefly, a solution of ethyl acrylate monomer (99%, Aldrich), 0.1 wt.% azobisbutyronitrile (99%, Fluka), and 2 wt.% ethylene glycol dimethacrylate (98%, Aldrich) was injected in a nylon fabrics template. The monomeric mixture was allowed to polymerize for 24h at 60ºC and post-polymerize for 24h at 90ºC. The materials were next washed to eliminate the porogen template. The resulting 1.6 mm thick scaffolds were thoroughly dried and punched into 1cm-diameter discs.

2.2. Preparation of HA solutions and coating procedure

Aqueous solutions of hyaluronic acid sodium salt (99%, Sigma, 1.63 MDa) in 0.2M sodium hydroxide (NaOH, extrapure, Scharlau) were prepared at 0.5, 1, 2 and 5 wt.% and stirred for 24h. These solutions were forced into the scaffolds pores by applying vacuum with a syringe and next thoroughly dried as described in [32]. After preparation, the hybrids were stored

under vacuum until use. Coated scaffolds will be designed as *y*HA*x*, where *y* is the concentration of the coating solution, and an *x* is added to the series of homologous crosslinked samples.

2.3. Crosslinking of HA coating

The HA coating of PEA scaffolds was crosslinked with divinyl sulfone (97%, Aldrich, 118.15 Da) in a series of samples. Firstly, 6 replicates of coated samples were immersed during 20 min in 5 mL of a 80/20 vol. mixture of acetone (synthesis grade, Scharlau)/0.2M (aq) NaOH with a pH of 11-12 adjusted with HCl (≥99.8%, Sigma-Aldrich). DVS was next added in a 1:0.9 molar ratio of DVS to HA monomeric units, dissolved in 1 mL of the acetone/NaOH solution. Samples were left in the solution for 24 h to ensure that the crosslinking reaction was completed. Next, samples were rinsed in a 20/80 vol. acetone/distilled water mixture for 30 min, followed by a washing with distilled water for 30 min, and dried as described.

2.4. Preparation of HA discs

In order to obtain HA discs to be used as control, hyaluronic acid sodium salt was dissolved in a NaOH (aq) 0.2 M solution to a concentration of 5 wt.% by gently shaking for 24 h and stirring at 200 rpm for 2 extra hours. Next, DVS was added and stirred at 300 rpm for 1 minute. 10 mL of the DVS/HA solution were poured into a 8.5 cm diameter Petri dish and the crosslinking reaction was let to occur for 24 h. The obtained gel was punched into 5 mm-diameter discs. The discs were washed 5 times for 24 h in a 50/50 vol. acetone/distilled water mixture, and dried in an oven at 40ºC for 5 h followed by 24 h under vacuum at room temperature. Samples were kept under vacuum and darkness until use.

2.5. Determination of the amount of HA entrapped in the scaffolds

The amount of HA entrapped in the scaffolds was quantified before and after its crosslinking by comparing the weight of bare samples with that after coating and after crosslinking, in all cases followed by drying. A Mettler AE 240 balance (Mettler-Toledo Inc., Columbus, OH, USA) was used for this purpose. These data allowed the estimation of the filling efficiency and the mass loss on account of crosslinking.

The amount of HA adsorbed on the scaffolds surface during the coating process and the HA remaining after crosslinking was quantified by the HA mass fraction in the scaffold, ω_{HA}, defined as: $\omega_{HA} = m_{HA}/(m_{HA} + m_{bare})$, where m_{bare} is the mass of bare scaffold and m_{HA} is the mass of dry HA coating. The relative loss during the crosslinking (HA_{loss}(%)) was determined as: $HA_{loss} = \frac{m_{HA\ initial} - m_{HA\ final}}{m_{HA\ initial}} \cdot 100$, where $m_{HA\ initial}$ is the mass of HA incorporated during the coating process and $m_{HA\ final}$ is the mass of HA remaining after the crosslinking step. Measurements were performed 3 times for each HA concentration.

2.6. Morphological observation

A JSM-5410 scanning electron microscope (SEM; JEOL Ltd., Tokyo, Japan) was used to characterize the obtained materials. Surfaces and inner sections of the samples (exposed by fracturing the samples previously frozen by immersion in liquid nitrogen) were observed after a sputter-coating with gold. The working distance was fixed at 15 mm and the acceleration voltage at 15 kV.

Samples swollen for 4 days (by immersion in phosphate buffer saline (PBS), by immersion in distilled water, or maintained in an atmosphere of PBS, PBS(RH)), were mounted on a specimen holder and immersed in nitrogen slush. Once frozen, these samples were transferred to a JSM 6300 microscope (JEOL Ltd., Tokyo, Japan) in the cryoSEM device. An inner section was then exposed by fracturing the sample, and ice sublimation started at -80ºC. After

40 min, samples were sputter-coated with gold and examined at 20 kV of acceleration voltage.

2.7. Samples lyophilization

Coated samples, previously swollen for four days in PBS, were frozen by immersion in liquid nitrogen for 10 minutes, and then lyophilized at -80ºC in a LyoQuest-85 (Telstar) during 24 h in order to preserve the morphology of the coating upon drying.

2.8. Composition determination by TGA

Thermogravimetric analyses (TGA) were performed in a TA SDT Q600 thermobalance (TA Instruments, New Castle, DE, USA) in order to determine the thermal degradation of the samples and estimate their composition. Three sets of samples were scanned: bare scaffolds, HA films and 5HAx constructs. Each set of samples was immersed in water or in PBS for 3 days, followed by a thorough drying. Specimens weighing around 11 mg were scanned from 25ºC to 1000ºC at 10ºC/min under a nitrogen flux of 50 mL/min. The determination of solid residues left by each of the components (HA xerogel and PEA scaffold, respectively) at 700ºC allowed, assuming additivity, to quantify the mass fraction of HA in the coated scaffolds.

2.9. Determination of water sorption

The water sorption capacity of the samples was evaluated by immersion in PBS, in triplicate for each composition. Samples were weighed vacuum-dried before the immersion and swollen at selected time points. The water content (*WC*) was determined as: $WC = \frac{W_t - W_0}{W_0}$; where W_t is the weight of each sample swollen at time *t* and W_0 is its weight as dry. The equilibrium water content (EWC) was considered as the final *WC* obtained, when no further weight variation was observed.

2.10. Compression tests

Mechanical compression tests were performed in an EXSTAR TMA/ss6000 device (Seiko Instruments Inc., Chiba, Japan). HA discs, bare scaffolds and those coated with HA were measured, 5 replicates per composition. Experiments were carried out in a chamber filled with PBS, with the samples previously swollen in PBS for 3 days. A preload of 1 g was applied followed by a loading rate uniformly distributed over the surface of 20 g·min^{-1} up to 450 g at room temperature. The compressive elastic modulus was obtained as the initial slope of the stress ($\sigma = \frac{F}{A}$) *vs*. strain ($\varepsilon = \frac{\Delta l}{l_0}$) curve in the linear deformation region. E_1 was defined as the slope of the stress-strain curve at a strain of 20%; a second modulus, E_2, was determined in the stress range between 0.1 and 0.12 kPa, and the unitary limit deformation, ε_l, was defined as the deformation at the intersection of this slope with the strain axis.

2.11. Protein loading and controlled release study

Bovine serum albumin (BSA) was used as a protein model to evaluate the potential of PEA scaffolds coated with HA as a controlled release system. Each sample (previously swollen in PBS) was loaded overnight at 37ºC in 1.2 mL of a 1 mg/mL BSA (Thermo Scientific)

solution in PBS. After absorption, samples were transferred to 1.2 mL of fresh PBS each to follow the protein release. The supernatants were collected at selected time points (up to 240 h) and replaced with fresh PBS tempered at 37ºC. Three replicates per time, material and treatment were measured.

The BSA concentration in each supernatant was determined with a Micro BCA Protein assay kit (Thermo Scientific) following the manufacturer's instructions, and its absorbance was read with a Victor Multilabel Counter 1420 spectrophotometer (Perkin Elmer, Waltham, MA; USA) at 570 nm.

2.12. Statistics

All the experimental data are given as mean ± standard deviation. Statistical assessment of significant variance was performed through a one-way ANOVA with the Statgraphics plus software (Statistical Graphics Corp., version 5.1, Princeton, NJ). Statistical tests were performed at 95% significance level (p-value<0.05).

3. Results

3.1. Efficiency of the coating process

The molecular weight between crosslinks within the PEA matrix of the scaffolds here prepared, M_{PEA}, can be theoretically determined as $M_{PEA} = \nu \cdot M_{EA}$, where ν is the number of monomeric units per chain, i.e., $\nu = n_{EA}/n_{chains} = n_{EA}/(n_{EGDMA} \cdot \varphi_{EGDMA}/2)$. Herein n_{EA} and n_{EGDMA} are the moles of EA and EGDMA, respectively, M_{EA} is the molecular weight of EA (100.12 g/mol) and φ_{EGDMA} is the functionality of the crosslinker, 4. Thus, the theoretically M_{PEA} results in a value of 5057.0 g/mol or, equivalently, around 50 EA monomeric units between crosslinks.

The efficiency of the crosslinking procedure was characterized by determining the amount of HA incorporated before and after its crosslinking, in the dry state (Figure 1). In contrast to other acrylates [34], PEA permits the free diffusion of hyaluronan into the pores, because of the free water contained in the large pores and the lack of bound water on the hydrophobic surface of the PEA scaffolds. The amount of HA before crosslinking was found to increase linearly with the concentration of the starting HA solution used, its mass fraction ranging from 0.12 for the 0.5 wt.% solution to 0.40 for the 5 wt.% one. The crosslinking step, which involves the soaking of samples in a water/acetone solution, resulted in the undesired non-negligible release of a certain amount of HA from the scaffold. The relative loss of HA during crosslinking was though increasingly lower as the HA amount in the scaffold increased. For instance, the scaffolds coated with the 0.5 wt.% solution lost nearly 61% of the initially adsorbed HA during the crosslinking, whereas in those coated with the 5 wt.% HA solution only 19% of the initial HA mass was able to diffuse.

3.2. Morphology of the composites

SEM images of the cross section of dry PEA scaffolds coated with different HA starting solutions are shown to present the coating typologies obtained, Figure 2. For the lowest concentration (0.5 wt %), only scattered small aggregates of HA seem to adhere to the pores surfaces and the structure of the bare scaffold is still easily observable. The average diameter of the pores is kept, 117±29 microns, and no significant differences between the pores analyzed in the inner cross sections and those at the surface can be found.

When coated with the 1 wt.% HA solution, the deposition of a thin uniform layer can be already detected in some regions of the scaffolds. Using the 2 wt.% solution, partially clogged pores can be seen. Following the same trend, with the 5 wt.% HA solutions, many pores exhibit a uniform thick layer coating the channels, some of them being completely clogged.

The HA surfaces, like those of PEA, are smooth in their dry state, showing no microporosity (image not shown).

The cryoSEM images of samples swollen by immersion in PBS show that as the HA mass fraction increases, the number of hollow pores decreases. This could be due to an improvement in the water diffusion towards the inner pores of the scaffold because of the presence of hydrophilic HA. However, the trace left by PBS when sublimated in the cryoSEM device disguises the HA gel structure, which cannot be distinguished from the residue left by water sublimation. In order to better observe the HA coating in its swollen state avoiding the PBS artifacts, samples were swollen in PBS(RH). As these are milder swelling conditions, the changes were more moderate. Samples coated with 05HAx, as well as when dry, only exhibit few aggregates of HA, whereas in the 1HAx ones, some pores with a uniform coating layer start to be detected. For higher concentrations, the effects are more evident: 2HAx samples exhibit some pores partially clogged, and entirely clogged pores are numerous in the 5HAx samples. In sum, no great differences in the morphology of the coatings were detected when the composites are dry or swollen in PBS(RH). Thus, the change in the volumetric swelling of samples under humid atmosphere is moderate, and hence this treatment could be useful to compare the *EWC* of non-crosslinked and crosslinked samples without any risk of coating dissolution; it is, though, limited to characterize the morphology of the HA hydrogel under the conditions that the hybrids will face upon implantation, because hydrogels display a much greater volume when immersed in liquid aqueous media.

To characterize the coatings swollen by immersion in PBS, avoiding the appearance of residues left by PBS during sublimation in the cryoSEM device, yet maintaining the swollen volume, specimens were lyophilized after three days of immersion, and then observed in conventional SEM. For the lowest concentrations of HA solutions, small unconnected regions are shown (05HAx) and only thin layers were found in 1HAx. As for the highest

concentrations, 5HAx, many pores are entirely clogged, whereas slightly less for the intermediate concentration, 2HAx.

3.3. Thermogravimetric analysis

The thermogravimetric analyses allowed the study of the thermal degradation profile of the combined system, but also an additional determination of the mass fraction of HA effectively incorporated to the scaffolds (Figure 3). HA exhibits the lowest onset temperature, and a broad main degradation step between 205ºC and 400ºC; the main degradation of the bare scaffold occurs between 340ºC and 410ºC. The thermogram of the composite lies between those of its components, and exhibits a very particular profile: the first part of its main degradation stage follows a trend similar to HA although shifted towards higher temperatures (it has its onset at 235ºC), and the second part matches accurately that of PEA scaffolds although leaving a different percentage of solid residues. Apropos of this, at 700ºC HA left 28.8% of its initial mass as solid residue, PEA scaffolds left 8% and the coated scaffold (PEA 5HAx) had a residue of 20.6%. The residues left by sets of materials thermodegraded after immersion in PBS were compared with the residues left by samples immersed in water (data not shown) and no significant differences were observed.

3.4. Swelling of hyaluronic acid as coating in the scaffolds

The equilibrium water content *(EWC)* of scaffolds coated with a set of HA solutions was compared to determine the effect of the coating topology on their swelling degree. Coating the scaffolds surface with HA has an impact on their swelling behaviour. When bare hydrophobic scaffolds are merely placed in PBS, only a small fraction of the liquid is capable to penetrate into the pores (1.17). A significant increase of the *EWC* occurs when the scaffolds are coated with HA solutions; even when the lowest concentration is used, the water

content triples that of the bare scaffold. The *EWC* resulted to be independent of the starting solution used, suggesting that the mere presence of small amounts of HA improves water diffusion and the wettability of the scaffold; however, a plausible limitation of water uptake due to the confinement of the swollen hydrogel in the channels [32] seems to affect the 5HAx *EWC* in the sense of slightly decreasing it.

3.5. Mechanical properties

The influence of the hydrated coating on the mechanical performance of PEA scaffolds was followed by compressive tests. Swollen HA bulk discs and bare scaffolds were used as control, and their stress-strain profiles are represented along with those of coated scaffolds, Figure 5.

All curves show a similar convex trend with stiffness increasing progressively as the sample is deformed, ending with a densification regime. As expected, the swollen HA discs have the lowest compressive stiffness and the greatest deformability. The hybrids coated with the least concentrated solutions (0.5 and 1 wt.%), show slightly greater initial compressive moduli than the bare scaffold (18.2 and 20.1 kPa, respectively, *vs*. 17.7 kPa for the latter). A greater increase is observed for scaffolds coated with more concentrated solutions (2HAx and 5HAx), reaching moduli that nearly double that of the bare scaffold (32.26 and 33.4 kPa, respectively). This increase is proportional to the amount of HA incorporated, although the modulus of the HA gel (11.5 kPa) is lower than that of the hydrophobic scaffold.

The change in the tendency observed in the curves occurs at a strain of approximately 75% for the bare scaffolds, which is close to its porosity, and at lower strains for the coated ones: up to 50% for those coated with the more concentrated HA solution. As for the final modulus, the scaffolds coated with high HA concentrations (2 and 5 HA wt.% solutions) show lower moduli than the rest (909.4 and 835.4 kPa), as well as more gradual change of slope. The

hybrids coated with 0.5 and 1 wt.% solutions exhibit moduli close to that of the bare PEA scaffold (1.169 and 1.293 MPa, respectively, *vs.* 1.286 MPa for the latter). The HA discs show again the lowest value in this zone, 380 kPa.

The greater values of unitary limit deformation are those obtained for the controls: non-porous HA gel discs and bare PEA scaffolds (having the highest porosity). For the hybrids, a clear trend is observed: the higher the HA mass fraction (*i.e.* scaffolds coated with more concentrated HA solutions), the lower the extreme strain value.

3.6. Controlled release

Great differences were found among the amounts of BSA loaded in scaffolds, and HA discs: the latter were capable to adsorb almost three times more protein per mg of sample. As Figure 6 shows, no significant differences were found between bare and coated scaffolds in respect of the amount of BSA effectively loaded.

Figure 7 shows the curves of accumulated percentage of BSA released, M_t/M_0, for the loaded composite, PEA scaffolds and HA controls, where M_0 is the initial (loaded) mass of BSA in each material and M_t is the mass released from it at each time t. All materials present a similar trend, where two release regimes can be identified. A burst takes place at the beginning, lasting 8 hours, where a significant fraction of protein is released: up to 24% from HA discs, 52% from coated scaffolds, and 68% from bare ones. Next, a more sustained release follows up to the end time of the study, covering 47% from HA gel, 85% from PEA scaffolds and 65% from 5HAx coated PEA scaffolds after 12 days. In no case the total amount of BSA incorporated could be released.

Despite the similarities with respect to the shape of the curves, the single and hybrid materials exhibit indeed different behavior. Bare PEA provides a fast release of the loaded protein,

whereas HA gel provides a much more moderate rate of release, although also presents an initial burst, and the hybrids exhibit an intermediate behavior between its components, reaching much higher values in the initial burst than HA, but a slower rate in the second regime.

4. Discussion

The combination of PEA scaffolds with HA aqueous solutions was not trivial given the hydrophobicity of the former and the viscosity of the latter. A procedure allowing the production of different coating typologies was previously presented in [32]. It consisted in the use of HA aqueous solutions containing NaOH to reduce its viscosity [35] together with assisting the filling by applying vacuum. Scaffolds made of hydrophobic materials of different nature such as PLLA [36] and PCL [37] have also been coated with HA, but the effect of the concentration of the starting solution on the typology of the coating had not been followed systematically. Further, the procedure to obtain different coating typologies in thicker scaffolds in only one coating step by varying HA concentrations has been developed in this work.

The coating efficiency experiments showed that the higher the concentration of the HA solution used, the greater the amount of HA incorporated within the pores, as expected. However, as these coatings are soluble in water, a crosslinking step with DVS (which includes a swelling in an acetone/NaOH(aq) solution) was followed. During this step, the greater the HA mass fraction in the sample the lower the HA loss. A plausible explanation could be found in the HA ability to swell in water. Those samples coated with the lowest HA concentration only exhibit small aggregates inside the pores; thus, HA can swell with no restrictions but those imposed by the polymeric network. This great volume increase could lead to the detachment of the aggregates from the surface. If there is no impediment blocking

the pores, the detached piece of HA can easily circulate through the microchannels and eventually come out. Oppositely, in samples coated with more concentrated solutions, a greater amount of HA was adsorbed within the pores and because of the constrained swelling already described for this system in [32], HA exhibits a more restricted swelling limiting its detachment. Even more, if HA is swollen, as increases its volume, it could act as a top blocking the channels and avoiding the detached HA to come out from the pores. Thus, HA hydrogels remain constrained against the pores surfaces; nonetheless, such swelling does not provide a better interaction with the scaffold, due to the different chemical nature of both components. This fact can be observed on the SEM and cryoSEM images of 5HAx samples (Figure 2), where HA shows detached from PEA.

The use of thicker scaffolds than those used in [32] intended the fine augment of ω_{HA} without increasing the number of applied cycles, ensuring more uniform coatings throughout the thickness of the scaffolds in one step. Another consequence of using thicker scaffolds was the reduction on the amount of HA lost during crosslinking, because of a labyrinthine effect of the porosity. Indeed, the scaffolds used herein (produced from 16 layers of nylon meshes as porogen instead of 8) coated with a 5 wt.% HA solution reached, with a single cycle, an ω_{HA} equivalent to that reached by the 8-layered scaffolds after 5 loading-drying cycles with a 5 wt.% HA solution (those used in [32]). For HA solutions of 1 and 2 wt.%, the ω_{HA} attained with 16-layered scaffolds (0.071 and 0.143, respectively) is close to that of the 8 layers scaffolds after 1 cycle with 5% HA (0.148). Thus, for thinner scaffolds, the HA fraction remaining in the pores after the crosslinking step is thickness-dependent.

The thermogravimetric analyses provided values of solid residue that allowed to quantify the HA mass fraction in the coated scaffolds in an alternative way. A ω_{HA} of 0.36±0.05 was obtained for the PEA scaffold coated with 5HAx. This value is in good agreement with that obtained by weighing the samples before and after the coating (Figure 1), being 0.36±0.01.

The shift on HA's main thermodegradation stage towards higher temperatures of the hybrids can be attributed to an increased difficulty for the diffusion of the HA volatiles in the presence of the polymer matrix.

In order to modulate the thickness of the coating layer, the concentration of the HA solution was varied. As a result, HA coatings with topologies ranging from scattered aggregates up to completely clogged channels, with a uniform coating for the intermediate situations, were obtained. However, SEM micrographies gave limited information of the hybrids, as samples are observed in their dry state whilst their intended use is under aqueous (physiological) conditions. Observing the samples in their swollen state was not though exempt of difficulties: the cryoSEM technique hid the results (because of a PBS excess) of porous samples previously immersed in PBS (Figure 2) and prevented to differentiate the PBS traces from the swollen HA in the pores. To overcome this artifact, micrographies of a set of samples swollen in PBS(RH) were taken; in this case there is no surrounding water that could be mistaken for the swollen HA structure. However, since these swelling conditions are milder, the degree of swelling is lower than in samples immersed in aqueous media and these results are not extensive to physiological conditions. When samples swollen in PBS were observed with conventional SEM after lyophilization, the scaffolds coated with 2 and 5% HA solutions exhibited pores practically clogged by the swollen HA. For the lowest concentrations, either only limited areas are coated (05HAx), or at most some pores start to be clogged (1HAx). The similarities between the 2HAx and 5HAx could be attributed to the constrained swelling experienced by HA for the highest fractions, revealed upon swelling (Figure 4). This phenomenon was reported for samples swollen in 66% RH in [32].

The elastic modulus increases with the HA fraction (Figure 5). This effect can be attributed to the greater difficulty in extruding water from the HA gels than from the void scaffolds pores. Constrained swelling aside, for the scaffolds coated with the most concentrated solutions, a

greater amount of HA lodging water within the network occupies the scaffold pores and thus lesser water can flow freely through them, *i.e.*, the gelled state of HA impedes such flow. This phenomenon, known as poroelasticity, occurs when porous materials filled with liquids are compressed, because of the incompressibility of the latter [38]. As a result, even if the HA modulus is lower, it increases the elastic modulus nearly two-fold that of the bare scaffold as it hinders the flow of water entrapped in the hydrogel. A similar reinforcing role has been described in other combined systems [39,40]. The presence of increasing fractions of HA within the pores increases the stresses needed to reach a certain strain. As can be observed in the second linear region in the stress-strain plot (E_2 has been determined in the stress interval between 100 and 120 kPa, except for HA, for which it has been determined at lower stress levels), the scaffolds coated with concentrated HA solutions are less deformed given the same value of stress. This is an indicator that the smaller lumen of the filled pores are subsequently sooner collapsed. This second modulus, obtained after pores collapse, decreases as PEA is combined with HA, because here both materials are simultaneously compressed and the HA modulus is lower when it is swollen. For the scaffolds coated with 05HAx and 1HAx, values similar to those reached by the bare scaffolds were obtained, in agreement with this rationale.

The feasibility of using the combined system composed of a PEA scaffold and HA filling as a protein (or other molecule) delivery platform was assessed in the controlled release study. The loaded BSA molecules might be lodged in different locations depending on the considered material. In HA discs, the protein could be either adsorbed on the surface or embedded in the polymeric network. In bare scaffolds, BSA can be either adsorbed on the surface, or in the liquid filling the pores. The BSA present in the hybrid scaffold would be lodged in a combination of the aforementioned locations.

The BSA release was found to exhibit two regimes (Figure 7): the initial burst that occurs within 8 hours, and a more sustained release up to 12 days. The initial solute release regime

from HA discs and 5HAx coated PEA scaffolds can be fitted to the simple exponential relation according to [41] and [42]; $M_t/M_0 = k \cdot t^n$, where M_t/M_0 is the fractional solute release, t is the release time in hours, k is a constant characteristic of the macromolecular network system, and n is the diffusional exponent characteristic of the release mechanism [41]. The model was not applied to bare scaffolds because of their high initial release suggesting that the HA component is the vehicle for a sustained release. For HA the equation gives $M_t/M_0 = 0.1194 \cdot t^{0.33}$ (R^2=0.9944) and for 5HAx it is $M_t/M_0 = 0.2269 \cdot t^{0.33}$ (R^2=0.9784). The fact that the best fit is obtained for an *n*=0.33 in both cases, below the limit of 0.43 that is attributed to pure Fickian diffusion, indicates that the diffusion mechanism taking place is not Fickian, *i.e.,* other factors besides pure diffusion are taking part in this process. These mathematical models are widely used to describe solvent release from hydrogels, where *k* is interpreted as a structural/geometric factor to account for the different tortuosities of the transport path [42]. This could explain why the value obtained for the hybrids is higher than that of HA discs.

Given the highly hydrophilic and swellable nature of HA discs, changing from a loaded solution to a non-loaded one could lead to not only a release of the model protein but also a non-negligible swelling of the polymeric network because of the greater water activity in the medium. Thus, the model developed by Ritger and Peppas specifically for swellable devices might be used [42]. In such case, $M_t/M_0 = k_1 \cdot t^n + k \cdot t$ applies, which when generalized for alternative geometries implies $k = 1 - (1 - k_2 \cdot t)^n$. The following equation is achieved: $M_t/M_0 = 0.112602 \cdot t^{0.33} + (1 - (1 - 0.003741 \cdot t)^{0.33})$. With this approach the k_1 value is very close to the one obtained with the simple exponential relation; hence the resulting model is like the one obtained for the simple exponential diffusion, plus an extra term associated to the material swelling.

The second release regime exhibits an almost linear profile, which can be fittted to the linear equation $M_t/M_0 = k \cdot t + a$, where a accounts for the initial release and k for the linear growth of the amount released with time. For HA the fitting is $M_t/M_0 = 0.0006 \cdot t + 0.2935$, for 5HAx it is $M_t/M_0 = 0.0004 \cdot t + 0.5469$ and in this case also the data of bare scaffold could be fitted: $M_t/M_0 = 0.0005 \cdot t + 0.7101$. The greater a value is obtained for the scaffold, which is indicative of its more pronounced initial release. The fastest second regime release was observed for HA, which precisely had the highest k value in the fitted equation.

Previous works reported that negatively charged proteins are sustainably released from HA hydrogels after an initial burst; meanwhile, the release of positively charged proteins is interrupted after the initial rapid release due to electrostatic interactions with HA functional groups [43]. At the pH of this experiment, 7.4, BSA was above its isoelectric point (4.7) [44], and negatively charged. The results obtained for HA and 5HAx constructs, exhibiting an initial burst followed by a sustained release are in good agreement. However, other factors besides interaction of BSA with HA need to be taken into account, for instance the porosity; in the case of bare scaffolds and 5HAx coated ones, the BSA lodged in the free PBS filling the pores could contribute to the fast release, as it can diffuse easily to the surrounding medium.

5. Conclusions

PEA grid-like scaffolds coated with HA gels were prepared with the aim of developing hybrid systems composed of materials of very different nature: on the one hand, the hydrophobic acrylic polymer and on the other the highly hydrophilic and water-soluble (if not crosslinked) HA. The typology of the pore coatings can be accurately tailored by varying the HA concentration of the solution, ranging from scattered aggregates up to totally clogging the

pores. After injection, the solution can be effectively crosslinked with DVS *in situ* to increase its stability in aqueous environments. The efficiency of this step is highly dependent on the hybrid composition, in the sense of increasing with the HA fraction, since it gives rise to an impaired diffusion of chains out the pores during the crosslinking.

The incorporation of crosslinked HA in the microchannels enhances the mechanical performance of the scaffolds and increases their water uptake, which might favor the diffusion of substances along the channels. All in all, these hybrid systems combine the interesting biological properties of the antagonist polymers HA and PEA and allow the controlled release of substances by diffusion through the gel coating from an otherwise hydrophobic scaffold; in this sense, these materials might find further applications in the tissue engineering field.

Acknowledgements

The authors acknowledge the financing through projects FP7 NMP3-SL-2009-229239 (RECATABI) and MAT2011-28791-C03-02 and -03. This work was also supported by the Spanish Ministry of Education through M. Arnal-Pastor FPU2009-1870 and M. Pérez-Garnes BES-2009-015314 grants.

References

[1] M. Pérez Olmedilla, N. Garcia-Giralt, M.M. Pradas, P.B. Ruiz, J.L. Gómez Ribelles, E.C. Palou and J.C. Monllau-García, Biomaterials, 27 (2006) 1003.

[2] P. Rico, J.C. Rodríguez Hernández, D. Moratal, G. Altankov, M. Monleón Pradas and M. Salmerón-Sánchez, Tissue Eng. Part A, 15 (2009) 3271.

[3] A.J. Campillo-Fernández, R.E. Unger, K. Peters, S. Halstenberg, M. Santos, M. Salmerón-Sánchez, J.M. Meseguer Dueñas, M. Monleón Pradas, J.L. Gómez Ribelles and C.J. Kirkpatrick, Tissue Eng. Part A, 15 (2009) 1331.

[4] A.J. Campillo-Fernández, S. Pastor, M. Abad-Collado, L. Bataille, J.L. Gómez Ribelles, J.M. Meseguer Dueñas, M. Monleón Pradas, A. Artola and J.M. Ruiz Moreno, Biomacromolecules, 8 (2007) 2429.

[5] C. Martínez-Ramos, A. Vallés-Lluch, J.M.G. Verdugo, J.L.G. Ribelles, J.A. Barcia Albacar, A. Baiget Orts, J.M. Soria López and M. Monleón Pradas, J. Biomed. Mater. Res. Part A, 100 (2012) 3276.

[6] J.M. Soria, C. Martínez Ramos, M. Salmerón Sánchez, V. Benavent, A. Campillo, J.L. Gómez Ribelles, J.M. García Verdugo, M. Monleón Pradas and J.A. Barcia, J. Biomed. Mater. Res. Part A, 79 (2006) 495.

[7] J.M. Soria, C. Martínez Ramos, O. Bahamonde, D.M. García Cruz, M. Salmerón Sánchez, C. Casas, M. Guzmán, X. Navarro, J.L. Gómez Ribelles, J.M. García Verdugo, M. Monleón Pradas and J.A. Barcia, J Biomed Mater Res Part A, 83 (2007) 463.

[8] C. Martínez-Ramos, S. Lainez, F. Sancho-Bielsa, A. García Esparza, R. Planells-Cases, J.M. García Verdugo, J.L. Gómez Ribelles, M. Salmerón Sánchez, M. Monleón Pradas, J.A. Barcia and J.M. Soria, Tissue Eng 14 (2008) 1365.

[9] J.M. Soria, M. Sancho-Tello, M.A. García Esparza, V. Mirabet, J.V. Bagan, M. Monleón and C. Carda, J Biomed Mater Res Part A 97 (2011) 85.

[10] Y. Mei, K. Saha, S.R. Bogatyrev, J. Yang, A.L. Hook, Z.I. Kalcioglu, S.W. Cho, M. Mitalipova, N. Pyzocha, F. Rojas, K.J. Van Vliet, M.C. Davies, M.R. Alexander, R. Langer, R. Jaenisch and D.G. Anderson, Nat. Mater. 9 (2010) 768.

[11] J.C. Chachques, M.M. Pradas, A. Bayes-Genis and C. Semino, Expert Review Cardiovasc. Therapy, 11 (2013) 1701.

[12] J.L. Alió Del Barrio, M. Chiesa, G. Gallego Ferrer, N. Garagorri, N. Briz, J. Fernandez-Delgado, M. Sancho-Tello, C.C. Botella, I. García-Tuñón, L. Bataille, A. Rodriguez, F. Arnalich-Montiel, J.L. Gómez Ribelles, C.M. Antolinos-Turpín, J.A. Gómez-Tejedor, J.L. Alió and M.P. De Miguel, J. Biomed. Mater. Res. Part A, 103 (2015) 1106.

[13] C. Castells-Sala, A. Vallés-Lluch, C. Soler-Botija, M. Arnal-Pastor, C. Martínez-Ramos, T. Fernandez-Muiños, N. Marí-Buyé, A. Llucià-Valldeperas, B. Sanchez, J.C. Chachques, A. Bayes-Genis, M. Monleón Pradas and C.E. Semino, J. Mater. Sci., 42 (2007) 8629.

[14] A.V. Lluch, A.C. Fernández, G.G. Ferrer and M.M. Pradas, J. Biomed. Mater. Res. Part B, Applied Biomater., 90 (2009) 182.

[15] A. Vallés-Lluch, M. Arnal-Pastor, C. Martínez-Ramos, G. Vilariño-Feltrer, L. Vikingsson, C. Castells-Sala, C.E. Semino and M. Monleón Pradas, Acta Biomaterialia, 9 (2013) 9451.

[16] C. Martínez-Ramos, E. Rodríguez-Pérez, M.P. Garnes, J.C. Chachques, D. Moratal, A. Vallés-Lluch and M. Monleón Pradas, Tissue Eng. Part C, Methods, 20 (2014) 817.

[17] T. Ohara, T. Sato, N. Shimizu, G. Prescher, H. Schwind, O. Weiberg, K. Marten and Helmut Greim, in Wiley Ullmann's Encyclopedia of Industrial Chemistry, Wiley-VCH Verlag, Weinheim (Germany), 2000.

[18] R. Brígido Diego, M. Pérez Olmedilla, A. Serrano Aroca, J.L. Gómez Ribelles, M. Monleón Pradas, G. Gallego Ferrer and M. Salmerón Sánchez, J. Mater. Sci: Mater. Med. 16 (2005) 693.

[19] C. González-García, M. Cantini, D. Moratal, G. Altankov and M. Salmerón-Sánchez, Colloids Surf. B 111 (2013) 618.

[20] D. Vigetti, E. Karousou, M. Viola, S. De Leonibus, G. De Luca and A. Passi, Biochimica et Biophysica Acta, 1840 (2014) 2452.

[21] R. Stern, A.A. Asari and K.N. Sugahara, Eur. J. Cell Biol., 85 (2006) 699.

[22] N. Shoham, A.L. Sasson, F.H. Lin, D. Benayahu, R. Haj-Ali and A. Gefen, J. Mech. Behavior Biomed. Mater., 28 (2013) 320.

[23] M.N. Collins and C. Birkinshaw, J. Applied Polym. Sci., 104 (2007) 3183.

[24] A. Temiz, K.C. Kazikdas, B. Ergur, K. Tugyan, S. Bozok and D. Kaya, Otolaryngol Head Neck Surg 143 (2010) 772.

[25] A. Fakhari and C. Berkland, Acta Biomaterialia, 9 (2013) 7081.

[26] A. Migliore, F. Giovannangeli, M. Granata and B. Laganà B, Clin. Med. Insights Arthritis Musculoskelet. Disord. 3 (2010) 55.

[27] M.N. Collins and C. Birkinshaw, J. Applied Polym. Sci., 120 (2011) 1040.

[28] K.H. Bae, J.J. Yoon and T.G. Park, Biotechnol. Progress, 22 (2006) 297.

[29] K. Motokawa, S.K. Hahn, T. Nakamura, H. Miyamoto and T. Shimoboji, J. Biomed. Res. Part A, 78 (2006) 459.

[30] J.H. Park, H.J. Cho, U. Termsarasab, J.Y. Lee, S.H. Ko S-H, J.S. Shim, I.S. Yoon and D.D. Kim, Colloids Surf. B 121 (2014) 380.

[31] S.W. Kim, K.T. Oh, Y.S. Youn, E.S. Lee, Colloids Surf B 116 (2014) 359.

[32] M. Arnal-Pastor, A. Vallés-Lluch, M. Keicher and M.M. Pradas, J. Colloid Interfac. Sci. 361 (2011) 361.

[33] J.C. Rodríguez Hernández, A. Serrano Aroca, J.L. Gómez Ribelles and M.M. Pradas, J. Biomed. Mater. Res. Part B: Applied Biomater., 84 (2008) 541.

[34] S. Tavazzi, L. Ferraro, M. Fagnola, F. Cozza, S. Farris, S. Bonetti, R. Simonutti and A. Borghesi, Colloids Surf. B 130 (2015) 16.

[35] A. Maleki, A.L. Kjøniksen and B. Nyström, Macromol. Symp., 274 (2008) 131.

[36] J.C. Antunes, J.M. Oliveira, R.L. Reis, J.M. Soria, J.L. Gómez-Ribelles and J. Mano, J. Biomed. Mater. Res. Part A, 94 (2010) 856.

[37] M. Lebourg, J.R. Rochina, T. Sousa, J. Mano and J.L.G. Ribelles, J. Biomed. Mater. Res. Part A, 101 (2013) 518.

[38] E. Detournay and A.D. Cheng, Fundamentals of poroelasticity. In: C. Fairhurst C, editor. Comprehensive rock engineering: principles, practice and projects, vol.II, Analysis and design method, Pergamon, New York, 1993.

[39] Y. Gong, L. He, J. Li, Q. Zhou, Z. Ma, C. Gao and J. Shen, J. Biomed. Mater. Res. Part B: Applied Biomater., 82 (2007) 192.

[40] H. Zhao, L. Ma, Y. Gong, C. Gao and J. Shen, J. Mater. Sci. Mater. Med., 20 (2009) 135.

[41] P.L. Ritger and N.A. Peppas, J. Control. Release, 5 (1987) 23.

[42] P.L. Ritger and N.A. Peppas, NA. J. Control. Release, 5 (1987) 37.

[43] F. Lee, J.E. Chung and M. Kurisawa, J. Control. Release, 134 (2009) 186.

[44] S. Ge, K. Kojio, A. Takahara and T. Kajiyama, J. Biomater. Sci. Polym. Ed. 9 (1998) 131.

Figure captions

Figure 1: HA mass fraction, ω_{HA}, after the coating (left ordinate) and percentage of HA loss, HA_{loss}, after the crosslinking and purification processes (right ordinate).

Figure 2*:* SEM and cryoSEM micrographies of PEA scaffolds coated with HA solutions of different concentrations, in their dry state, swollen by immersion in PBS, swollen under PBS vapor atmosphere and swollen by immersion in PBS followed by a lyophilization step. Scale bar: 300 μm.

Figure 3: Thermogravimetric profiles of HA discs, bare PEA scaffolds and PEA scaffolds coated with 5HAx.

Figure 4: Equilibrium water content of bare and coated scaffolds immersed in PBS.

Figure 5: (A) Stress-strain curves of PEA scaffolds, HA gels and scaffolds coated with differently concentrated HA solutions and crosslinked. (B) Initial compressive modulus, E_1, (C) final compressive modulus, E_2, and (D) unitary limit deformation (defined as the deformation at the intersection of the fitting to the second linear region with the strain axis), ε_L. (*) differences are statistically significant; (#) differences are not statistically significant.

Figure 6: Mass of BSA incorporated in bare and HA coated scaffolds, and HA discs, per mass unit of sample.

Figure 7: BSA release curve in PBS from bare and 5HAx scaffolds, and HA discs: accumulated percentage of BSA released at time *t vs.* time. Inset: detail of the initial release.

Figure 1

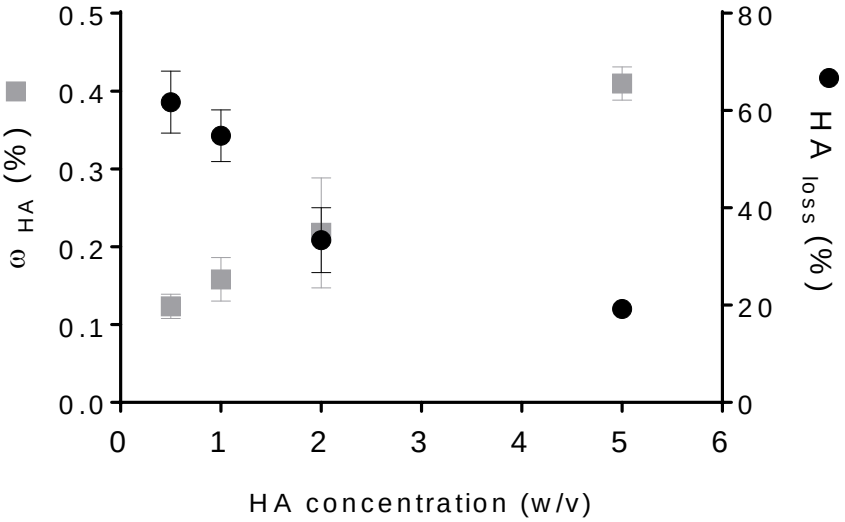

Figure 2

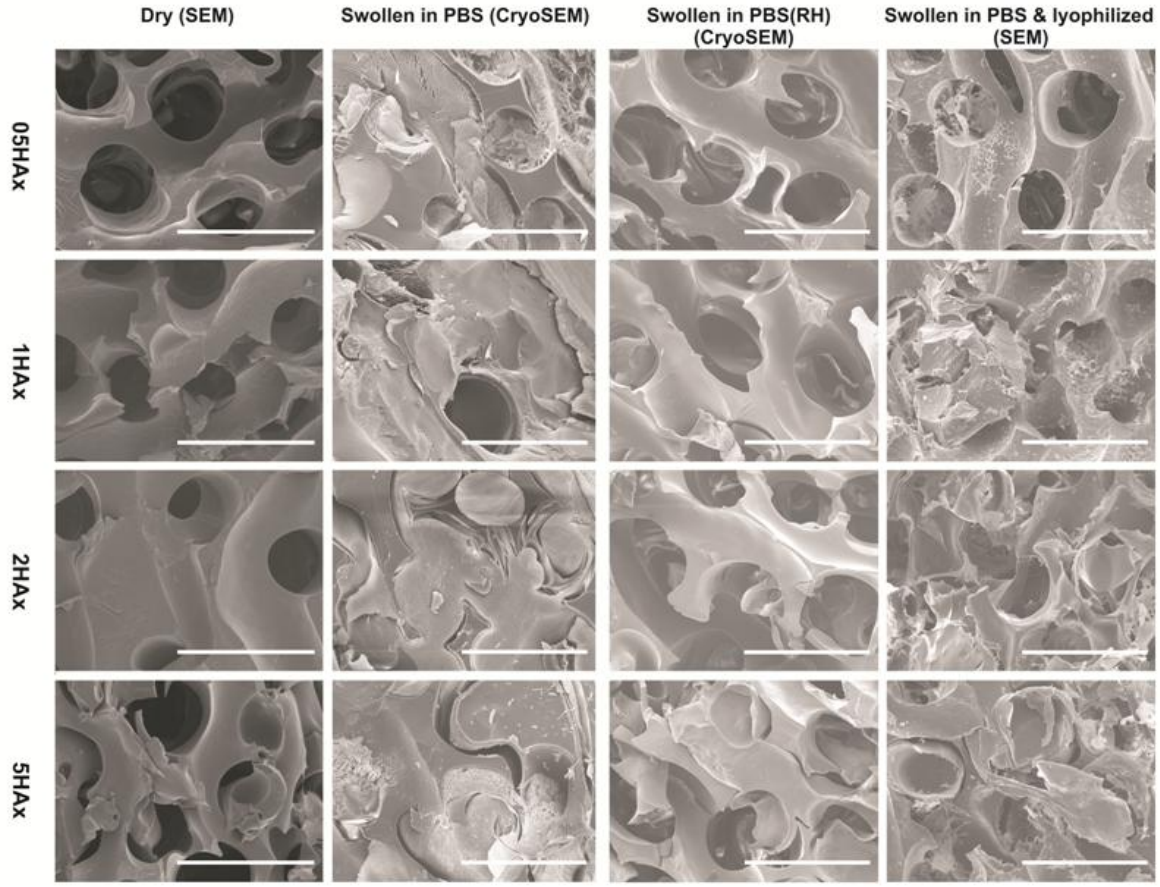

Figure 3

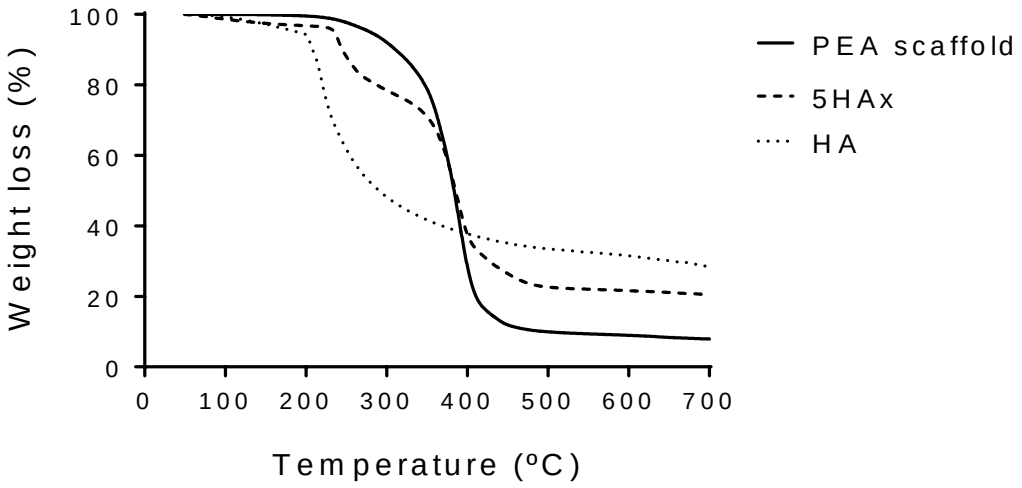

Figure 4

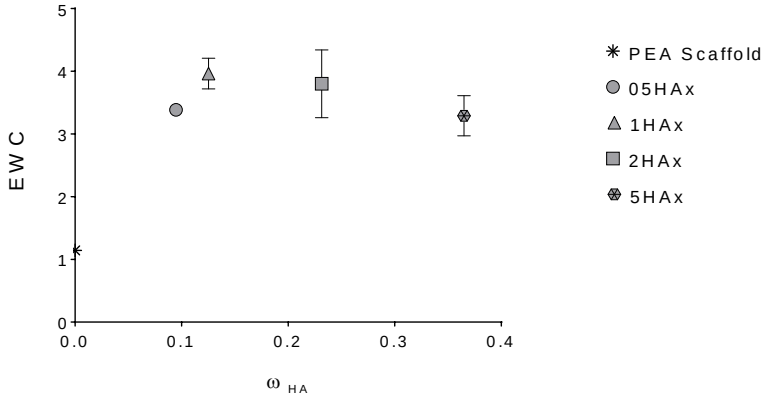

Figure 5

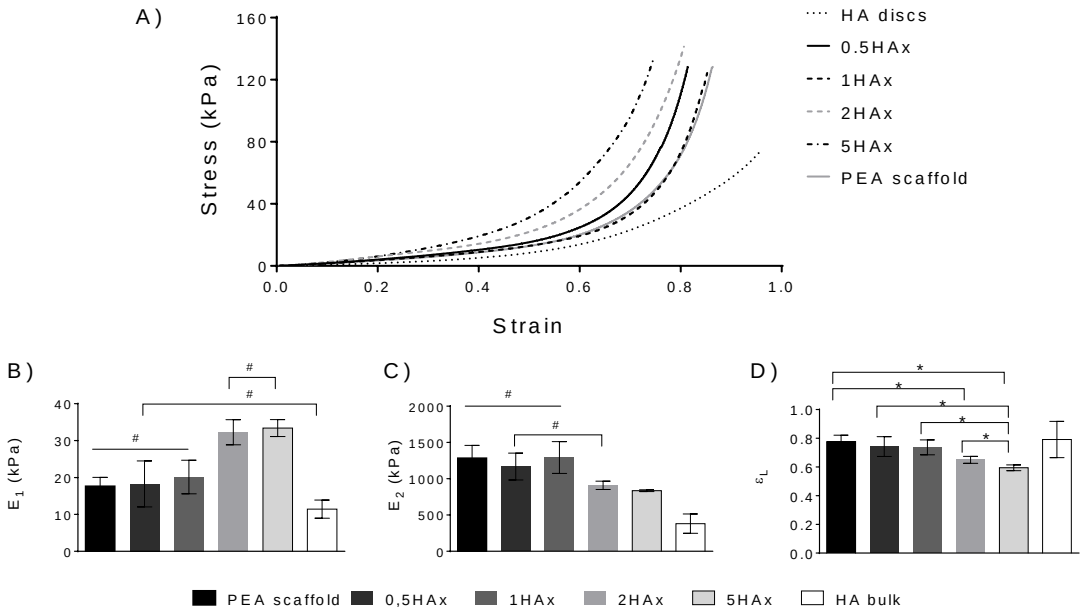

Figure 6

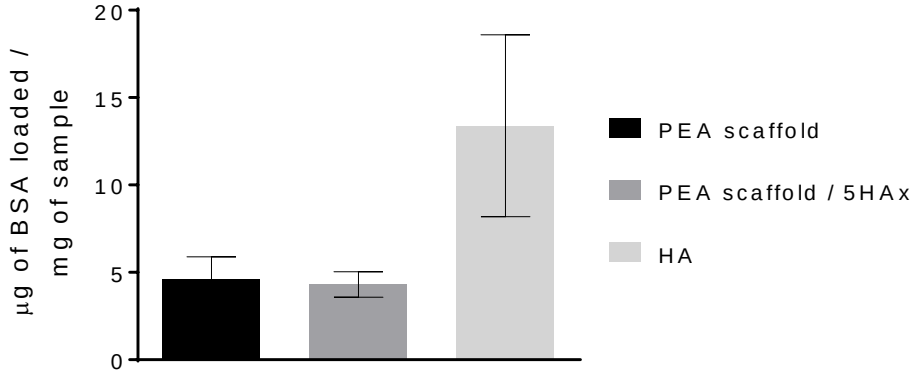

Figure 7

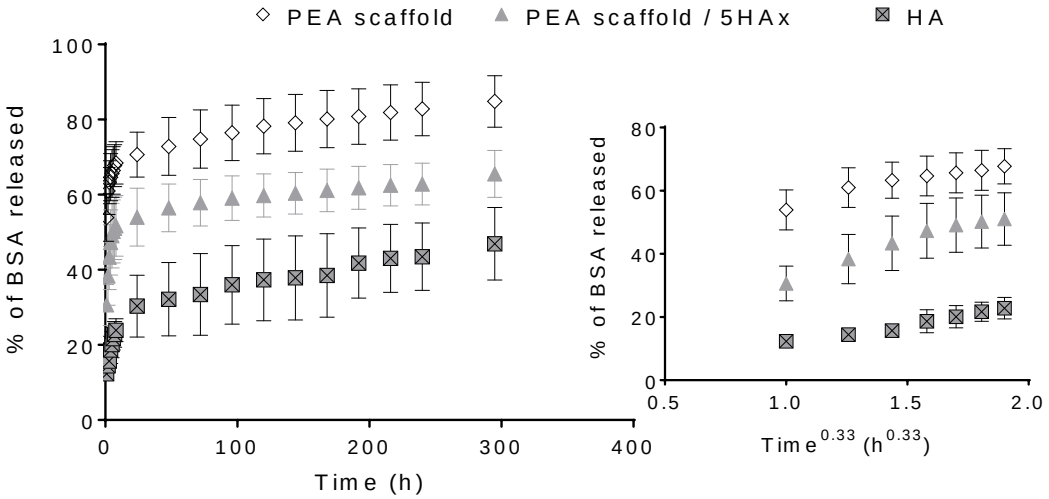
PEA scaffold
PEA scaffold / 5HAx
HA
% of BSA released
Time (h)
Time$^{0.33}$ (h$^{0.33}$)